A toolset for handling unstructured voronoi grids for MODFLOW

Published Version:
Bondua S., Bortolotti V., Macini P., Strpic K. (2023). A toolset for handling unstructured voronoi grids for MODFLOW. ENVIRONMENTAL MODELLING & SOFTWARE, 159, 1-11 [10.1016/j.envsoft.2022.105563].

Availability:
This version is available at: https://hdl.handle.net/11585/913586 since: 2023-02-02

Published:
DOI: http://doi.org/10.1016/j.envsoft.2022.105563

A toolset for handling unstructured Voronoi grids for MODFLOW

S. Bonduà*, V. Bortolotti, P. Macini, K. Strpić

*Corresponding author:

Stefano Bonduà

28 Via Terracini

40100 Bologna – Italy

E-mail: stefano.bondua@unibo.it

Software availability

Name of the software: VORO2MESH and TOUGH2Viewer

Developer: S. Bonduà

Contact address: stefano.bondua@unibo.it

Designed by: S. Bonduà V. Bortolotti, K. Strpić

First year available: 2020

Hardware requirement: PC

Software requirement: Windows OS

Program language: C++, Java.

Program size: VORO2MESH 475 kB (binary file); TOUGH2Viewer 20 MB (binary file)

Availability

- VORO2MESH: Freely available as a binary file at: https://site.unibo.it/softwaredicam/en/software/voro2mesh
- TOUGH2Viewer: Freely available as a binary file at: https://site.unibo.it/softwaredicam/en/software/tough2viewer. Source code is available at https://github.com/stebond/TOUGH2Viewer

Keywords

MODFLOW; TOUGH; unstructured grids; groundwater modelling; 3D; Voronoi

Abstract

MODFLOW is a modular hydrologic model developed by the United States Geological Service since 1984. The last version, MODFLOW 6, allows the use of finite volume (FV) general unstructured grid approach to solve the groundwater flow equations. The FV method entails constraints that are implicitly satisfied by a Voronoi discretization. In this paper, new versions of the freeware VORO2MESH and TOUGH2Viewer tools are presented for Voronoi grid generation for MODFLOW. Originally developed for the TOUGH family of codes, both software has been improved to also work with MODFLOW. VORO2MESH and TOUGH2Viewer have been applied to two case studies and the results have been compared with analytical solutions. Outcomes have demonstrated that VORO2MESH grids give simulation results very close to locally refined Grids created using the Quadtree approach; furthermore, the simulation activities are substantially enhanced using TOUGH2Viewer.

Keywords

Voronoi, MODFLOW, unstructured grids, TOUGH2Viewer, VORO2MESH, Paraview.

1 Introduction

Groundwater numerical modelling is nowadays one of the most used techniques for groundwater resource characterization. Numerical modelling implies the numerical resolution of the groundwater flow equations. Several finite difference (FD) software are available to the scientific community today. Among these, it is worth mentioning the Modular finite-difference flow model, MODFLOW, developed by the US Geological Survey (Harbaugh, 2005). MODFLOW is a command line software program written in Fortran. Unstructured grid capabilities have been introduced in 2013 in the MODFLOW-USG version (Panday et al., 2013). The use of unstructured grid allows for flexibility in grid design, can be used, for example, to focus resolution along rivers and around wells or to subdiscretize individual layers to better represent hydrostratigraphic units (Panday et al., 2013). In 2017 the general unstructured grid based on concepts developed for MODFLOW-USG has been implemented in MODFLOW 6 (Hughes et al., 2017).

As for spatial discretization, MODFLOW 6 can use a generalized control volume finite-difference (CVFD) formulation (the CVFD method is a type of the Finite Volume (FV) method, see, for example, (Bear and Cheng, 2010)), sometimes referred to as an integrated finite-difference method (IFDM). The CVFD formulation is therefore equivalent to the IFDM implemented in TOUGH2 (Pruess et al., 1999).

The FV diagram requires a geometric constraint on the grid blocks, in which each interface area between two blocks must be orthogonal to the segment connecting the two block nodes. MODFLOW 6 can use the ghost node correction method (Panday and Langevin, 2012) in order to correct the approximation introduced by the use of grids with non-orthogonal geometry. This allows local mass conservation. MODFLOW 6 can also use a Local Grid Refinement (LGR) approach (Mehl and Hill, 2013), as implemented, for example, in ModelMuse (Winston, 2009), that automatically generates the ghost node file to allow corrections for the MODFLOW 6 simulation results. Additionally, MODFLOW 6 allows application of the XT3D formulation approach for advanced capabilities to simulate three-dimensional anisotropy and dispersion and correct grid errors for cell connections that violate generalized CVFD assumptions (Provost et al., 2017).

MODFLOW simulation input files are in ASCII text format, while output files are in both ASCII and binary format. In the case of unstructured grids, MODFLOW 6 output files are limited to the binary format. File format details can be found in the MODFLOW 6 user manual (Hughes et al., 2017).

The MODFLOW numerical model contains the information about grid blocks, such as geometrical characteristics (area of the interfaces among blocks, volumes, etc.), flow and hydrodynamic parameters (porosity, permeability, etc), initial and boundary conditions. This information is stored in a set of input files, using a specified file format. Simple numerical models can be edited manually, but the need for increasing complexity and the use of very detailed numerical models necessitate the use of software tools to handle MODFLOW input files.

MODFLOW utility tools have also been developed to support Geological Information System (GIS) software to generate MODFLOW models directly from GIS data (Bittner et al., 2020; Gardner et al., 2018; Guzman et al., 2015; Park et al., 2019; Rossetto et al., 2019; Tian et al., 2018). Its popularity lead to a widespread utilization of MODFLOW in several fields and applications, e.g. as a Soil and Water Assessment Tool (SWAT) (Aliyari et al., 2019; Bailey et al., 2020; Chen et al., 2018; Maleki Tirabadi et al., 2021; Wei et al., 2019), and water pollution (Elsayed and Oumeraci, 2018; Esfahani et al., 2021) in which MODLOW has been coupled with MT3D (Bedekar et al., 2016).

In order to improve the numerical model creation task and visualization of the results, several commercial and free Graphical User Interface (GUI) tools for MODFLOW tools have been developed by the scientific community. A review of MODFLOW GUI can be found in (Hariharan and Uma Shankar, 2017).

Among the free tools for MODFLOW 6, it is worth mentioning ModelMuse (Winston, 2009), Freewat (Rossetto et al., 2019), and FloPy (Bakker et al., 2016). ModelMuse is a free and open source GUI for MODFLOW and related software developed by the U.S. Geological Survey (USGS). Freewat is an open source and public domain GIS integrated modelling environment for the simulation of water quantity and quality in surface water and groundwater with an integrated water management and planning module. FloPy is a Python Package for creating, running, and post-processing MODFLOW-Based Models. Among the commercial tools, it is worth mentioning Visual MODFLOW, Groundwater Modeling System (GMS), and Groundwater VISTAS. Visual MODFLOW is a commercial GUI for MODFLOW. It was introduced by the 'Waterloo Hydrogeologic' company in August 1994 (Hariharan and Uma Shankar, 2017). GMS is distributed from AQUAVEO. Groundwater VISTAS (Rumbaugh and Rumbaugh, 2011) is distributed by Environmental Simulations, Inc. (ESI), USA.

Table 1 reports a summary of the main characteristics of the above-mentioned tools for MODFLOW.

Software name	2D/3D Structured grids	2.5D Voronoi grids	Filter export for external viewer	Free	Commercial	Source Code Availability
Visual MODFLOW flex	YES	YES	NO	NO	YES	NO
GMS	YES	YES	NO	NO	YES	NO
Groundwater VISTAS	YES	YES		NO	YES	NO
ModelMuse	YES	NO	NO	YES	NO	YES
Freewat	YES	NO	YES	YES	NO	YES
FloPy	YES	NO	YES	YES	NO	YES

Table 1 – List of pre- and post-processors for MODFLOW 6.

As it can be noted from Table 1, currently there are no free tools for Voronoi grid generation and management for MODFLOW available for the scientific community. Voronoi grids implicitly satisfy the geometrical constraint of the FV computation, avoiding ghost node corrections and allowing local grid refinement without loss of accuracy. In literature, a growing number of algorithms and codes have been developed for Voronoi tessellation. Among them, we can find QHULL (Barber et al., 1996), PARAVT (González, 2016), voro++ (Rycroft, 2009), TetGen (Si, 2015), CGAL (The CGAL Project, 2018). These are general-purpose tools, and they need to be specifically adapted for a specific application.

The present paper illustrates application of a free toolset for MODFLOW 6 to generate unstructured Voronoi grids and to visualize simulation results obtained on unstructured Voronoi grids. The toolset is composed of two software programs, VORO2MESH (Bonduà et al., 2017) and TOUGH2Viewer (Bondua et al., 2012; Bonduà et al., 2017; Bonduà and Bortolotti, 2020), originally developed for the TOUGH family of codes.

This set of tests has unambiguously proven the effectiveness of the VORO2MESH and TOUGH2Viewer to improve MODFLOW numerical modelling.

2 Materials and Methods

The verification and validation of the two tools were performed by means of two case studies. Case study A compares the results of a 2D Darcy flow problem numerically modelled with a LGR (Mehl and Hill, 2013) and a Voronoi grid, created using VORO2MESH and edited in TOUGH2Viewer. Case study B compares the numerical simulations of the classic 2D quarter five-spot problem with a well-known analytical formulation.

Several LGR grids have been created with both ModelMuse and VORO2MESH tools. The workflow of the proposed tool set for the numerical simulation can be resumed in: (i) VORO2MESH grid generation; (ii) grid visualization and editing by using TOUGH2Viewer; (iii) MODFLOW numerical computation; (iv) TOUGH2Viewer results visualization. The flowchart of the workflow is shown in Figure 1.

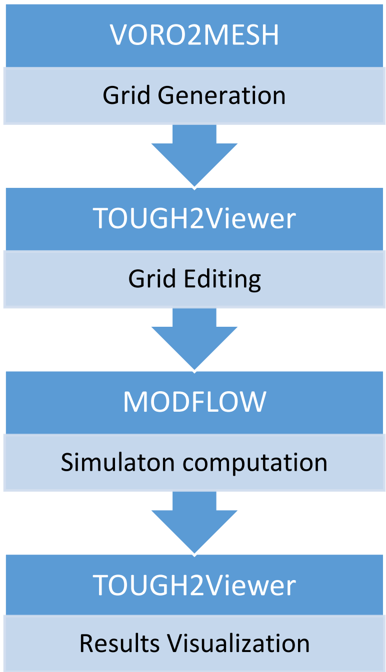

Figure 1 – workflow in using VORO2MESH and TOUGH2Viewer for MODFLOW.

2.1 VORO2MESH

VORO2MESH (Bonduà et al., 2017) is a command line utility software that allows the creation of fully 3D Voronoi tessellation of a convex domain. VORO2MESH is written in C++ and is based on the voro++ library (Rycroft, 2009). Basically, VORO2MESH can operate by using a set of seed points as inputs or it can generate the necessary seeds points by using a set of input surfaces representing the geological horizons. Originally developed for TOUGH grids, VORO2MESH has been improved with MODFLOW 6 grid generation capabilities. MODFLOW 6 does not allow the use of a fully 3D Voronoi discretization, but it allows 2.5D Voronoi grid generation. However, unstructured layers can be managed thanks to the ghost nodes approach used by MODFLOW 6 (see (Hughes et al., 2017)). The grid generated by VORO2MESH can be visualized and edited with TOUGH2Viewer. The current version of VORO2MESH for MODLFOW grid generation is limited to 2D models.

In this new VORO2MESH version, the MODFLOW 6 unstructured grid generation is activated by setting the specific keyword generate_modflow2D_disu=1 of the voro2mesh.par parameter file. The keyword IPRN_doubles will define the grid format as specified in Table 2.

Keyword	Default value	Code description
generate_modflow2D_disu	0	1: Activate MODFLOW grid generation
IPRN_doubles	2	Parameter for double format specification of the MODFLOW DISU grid. The DISU file, containing the area, thickness, bottom, top etc array of the blocks will be written as specified in the table:

<table>
<tr><td></td><td></td><td><table><tr><th>IPRN</th><th>Real format</th></tr><tr><td>0</td><td>10G11.4</td></tr><tr><td>1</td><td>11G10.3</td></tr><tr><td>2</td><td>9G13.6</td></tr><tr><td>3</td><td>15F7.1</td></tr><tr><td>4</td><td>15F7.2</td></tr><tr><td>5</td><td>15F7.3</td></tr><tr><td>6</td><td>15F7.4</td></tr><tr><td>7</td><td>20F5.0</td></tr><tr><td>8</td><td>20F5.1</td></tr><tr><td>9</td><td>20F5.2</td></tr><tr><td>10</td><td>20F5.3</td></tr><tr><td>11</td><td>20F5.4</td></tr></table></td></tr>
<tr><td>IPRN_int</td><td>0</td><td>Parameter for integer format specification for connection specification. The NJA array will be written as specified in the table:<table><tr><th>IPRN</th><th>Integer format</th></tr><tr><td>0</td><td>10I11</td></tr><tr><td>1</td><td>60I1</td></tr><tr><td>2</td><td>40I2</td></tr><tr><td>3</td><td>30I3</td></tr><tr><td>4</td><td>25I4</td></tr><tr><td>5</td><td>20I5</td></tr><tr><td>6</td><td>10I11</td></tr><tr><td>7</td><td>25I2</td></tr><tr><td>8</td><td>15I4</td></tr><tr><td>9</td><td>10I6</td></tr></table></td></tr>
</table>

Table 2 —Option values for VORO2MESH grid generation. See Appendix A for an example of the generated file format.

VORO2MESH generates a turnkey set of input files for MODFLOW:

- flow.disu: is the classic MODFLOW ASCII DISU (Unstructured discretization) file. It contains the reference to the following files, each containing specific data values of the grid blocks:
  - flow.disu.area.dat: the horizontal projected block area;
  - flow.disu.bottom.dat: the elevation of the bottom block face;
  - flow.disu.top.dat: the elevation of the top block face;
  - flow.disu.cl12.dat: the array containing connection lengths between the centre of cell n and the face shared with each adjacent m cell;
  - flow.disu.hwva.dat: a symmetric array of size NJA. For horizontal connections, entries in HWVA are the horizontal width perpendicular to flow. For vertical connections, entries in HWVA are the vertical area for flow;
  - flow.disu.ihc.dat: an index array indicating the direction between node n and all of its m connections;
  - flow.disu.ja.dat: a list of cell number (n) followed by its connecting cell numbers (m) for each of the m cells connected to cell n;

where:

- NJA (from the MODFLOW manual (Langevin et al., 2017) is the sum of the number of connections and nodes, including n to m and m to n, and the total number of cells;
- HWVA (from the MODFLOW manual (Langevin et al., 2017) is a symmetric array of size NJA. For horizontal connections, entries in HWVA are the horizontal widths perpendicular to flow. For vertical connections, entries in HWVA are the vertical areas for flow;

- m and n: two connected cells.

An example of the output file is reported in Appendix A, referring to the grid in Figure 4.b.

In this work, the seed points are generated outside VORO2MESH in the case of structured Cartesian grids; in the case of unstructured grids, the seed points are computed by VORO2MESH, using a Centroidal Weighted Voronoi Tessellation (CWVT) approach.

2.2 TOUGH2Viewer

TOUGH2Viewer is originally developed for simulation result visualization of TOUGH codes which use the Integral Finite Difference Method (IFDM), a FV method, to solve governing heat and mass balance equations. TOUGH2Viewer is not only a viewer but it allows modification of grid block proprieties, boundaries and initial conditions through intuitive GUI. In the scope of presented work, TOUGH2Viewer capabilities have been extended allowing the visualization of MODFLOW 6 simulation results and modification of grid block proprieties, boundaries and initial conditions. TOUGH2Viewer is written in Java and uses the Java3D library for 3D rendering of finite volume grid models. Regarding TOUGH2Viewer MODFLOW 6 visualization capabilities, TOUGH2Viewer can read DISU output files (binary format) and DISV grid files.

The input files needed for a MODFLOW 6 DISU or DISV grid visualization are:

- tough2viewer.dat file: the file generated by VORO2MESH during DISU grid generation. It contains the geometric information of the blocks, such as node coordinates, number of vertices, vertex coordinates, face vertices index, etc. A detailed explanation of the tough2viewer.dat file can be found in (Bonduà et al., 2017);
- Optionally, TOUGH2Viewer can also read DISV binary files for result visualization;
- HDS (or BHD) binary file: the hydraulic head file results generated by MODFLOW during a simulation run;
- GRB binary file: contains the flow between connected blocks;
- CBC binary file: contains the BUDGET information;
- IC: an ASCII file containing the initial conditions of the numerical model;
- CHD ASCII file: the constant head specification;
- NPF ASCII file: Node Property Flow (NPF) Package.

These files are read in TOUGH2Viewer by a dedicated GUI as shown in Figure 2.

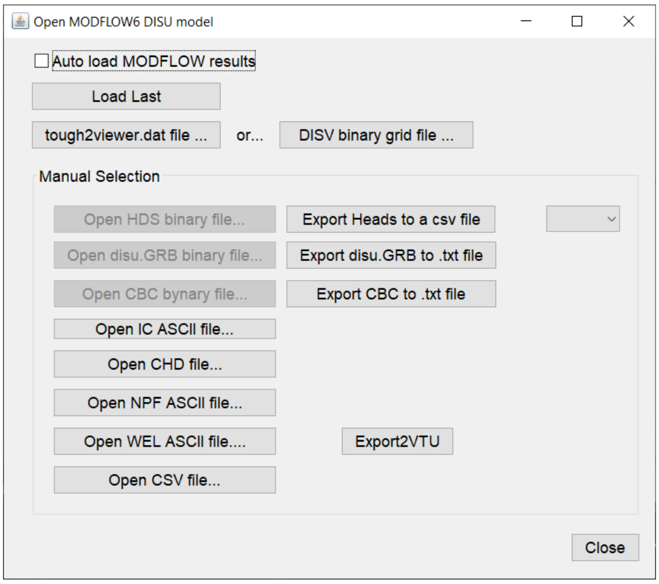

Figure 2 – MODFLOW6 DISU Model GUI: MODFLOW input/output files.

MODFLOW 6 simulation results can be directly visualized in TOUGH2Viewer or can be exported from TOUGH2Viewer in several formats, such as csv tables, txt files, or in Paraview[1] file format (vtu) (Ahrens et al., 2005), allowing an enhanced 3D model visualization (see Figure 3).

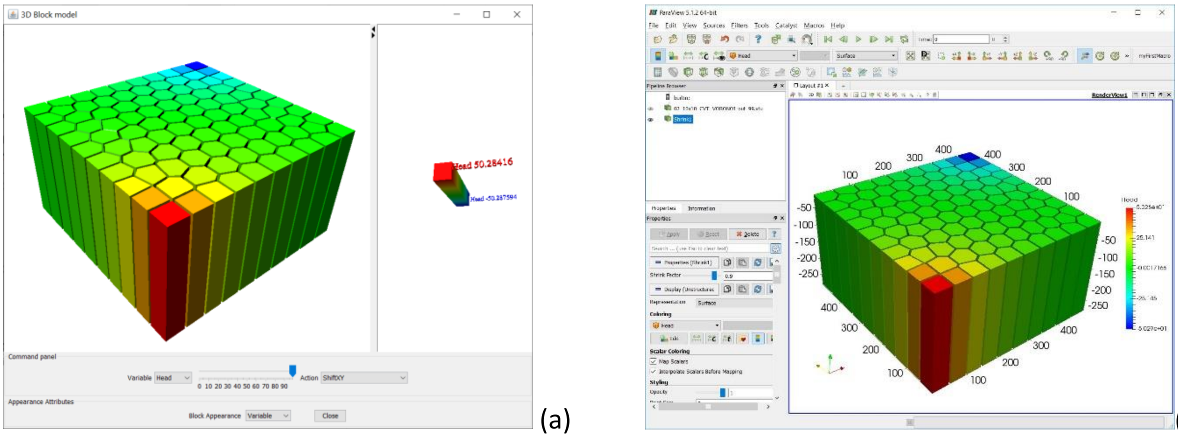

Figure 3 – (a) Model result visualization using TOUGH2Viewer; (b) the same model as (a) visualized in Paraview.

2.3 Case studies

2.3.1 Case A: the 2D Darcy flow

This case study consists of two-dimensional, confined groundwater steady state flow in an homogenous aquifer, as described in (Panday et al., 2013). The domain size is 700 x 700 x 100 m^3. The case study is analysed by using three grids. The first one (01_Darcy_quadtree) is a quadtree grid and it belongs to the example data set included with the MODFLOW distribution. It is composed of two nested grids: a coarse and a fine grid. In the coarse grid, the element size is 100 x 100 x 100 m^3, while in the fine grid element size is 33.33 x 33.33 x 100 m^3 (see Figure 4.a). The second grid (02_Darcy_quadtree_NO_GNC) has the same geometry as the first grid above, but it does not use the ghost node correction (GNC). The third grid (03_Darcy_Voronoi) is a Voronoi grid generated by VORO2MESH. The seed points used for the tessellation have the same coordinates as the cell centres of the nested grid (see Figure 4.b).

Boundary conditions have been set using the prescribed head boundary package in MODFLOW, by setting the elements at coordinate of x= 50 m, a constant head of 1.0 m, while elements at coordinate of x=650 m a constant head of 0.0 m. The permeability is 1.0 m/s. The numerical solutions are compared with the available analytical solution.

[1] http://www.paraview.org [Last access: 2022-09-29]

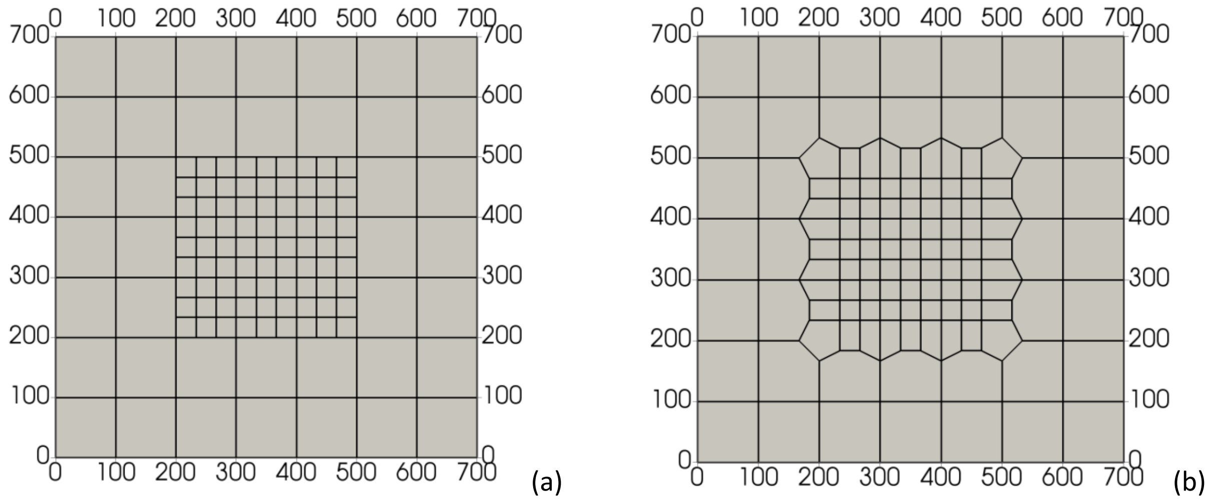

Figure 4– Discretization of the domain using: (a) nested grids; (b) the Voronoi grid. Visualization with Paraview.

2.3.2 Case B: The 2D quarter five-spot problem

In this case study, we used the classic five-spot scheme. In the case of a totally penetrating well in an confined aquifer, an analytical solution for the computation of the hydraulic head changes in space and time exists (Theis, 1935):

$$h_0 - h = \frac{Q}{4\pi h}\int_u^\infty \frac{e^{-a}}{a}\,\partial a, \text{ with } u = \frac{r^2 S}{4Tt}$$

where Q is the constant pumping rate, h the hydraulic head, h_0 the initial hydraulic head, t the time since pumping has begun, r the radial distance from the pumping well, S the storativity coefficient.

The five-spot problem is defined as an infinite set of injection and production wells in a staggered pattern (see Figure 5). The injection and production wells were arranged on a regular staggered grid of infinite extent. In this configuration, the superposition effects of the Theis solution can be applied. For symmetry reasons, it is sufficient to consider a quarter of the total five-spot domain. A Dirichlet boundary condition with zero flow was used for lateral surface of the square domain. Initial condition of the entire model has been set to hydraulic head equal to 0.0 m.

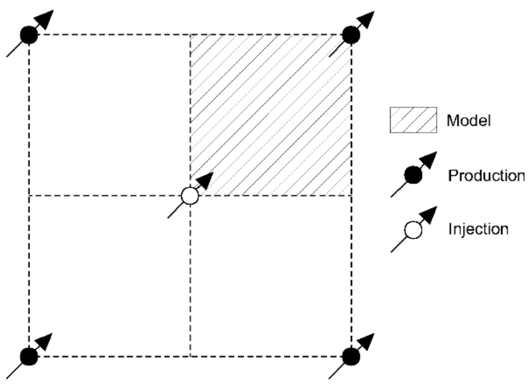

Figure 5– The five-spot problem conceptual model.

The analytical pressure state has therefore been computed for a quarter domain applying the superposition effect of a theoretically infinite (but in practice limited to 500 x 500 elements) staggered set of injection/production wells in the 500.0 x 500.0 m^2 square domain with a volumetric flow rate of 4.0 m^3/s.

The parameters of the model are given in Table 3.

Variable	Value

Hydraulic conductivity (m/s)	1.0E-4
Specific Storage (m^{-1})	1.0E-5
Aquifer thickness (m)	300.0
Staggered Size (m)	500.0
Time of injection/production (s)	43200 (12 hours)

Table 3 – Hydrodynamic parameters and model properties.

In order to verify and validate the toolset code, the five-spot problem has been simulated using different grid types: structured LGR, and unstructured Voronoi grids.

Table 4 summarizes the generated grids. The 01_structured (Figure 6.a), 02_Voronoi (Figure 6.b), 04_Voronoi_wells_refined (Figure 6.d), and 06_Voronoi_wells_line_refined (Figure 6.f) have been generated using VORO2MESH. The 03_Quadtree_wells_refined (Figure 6.c) and 05_Quadtree_wells_line_refined (Figure 6.e) have been generated by using ModelMuse Version 4.0.0.0. The 01_structured grid (Figure 6.a) is a 10x10 structured grid composed of 100 blocks of the same size/volume. The 02_Voronoi (Figure 6 .b) grid is composed of 100 grid blocks in which the blocks near the two wells have the same position as the 01_structured grid, and the other blocks satisfy the Centroidal Voronoi Tessellation (CVT) definition (the seed nodes are the centres of mass of the generated Voronoi blocks) (Du et al., 1999). The 03_Quadtree_wells_refined grid (Figure 6.c) is a quadtree grid obtained with a level 6 quadtree refinement. The 04_Voronoi_wells_refined grid (Figure 6.d) has the same number of blocks as the 03_Quadtree_wells_refined (Figure 6.c), but the remaining elements follow the weighted CVT approach (WCVT) (Inaba et al., 1994). The 05_Quadtree_wells_line_refined (Figure 6.e) grid is similar to the 03_Quadtree_wells_refined grid, but there is a non-symmetrical grid distortion along a line. The 06_Voronoi_wells_line_refined grid has the same number of grid blocks as 05_Quadtree_wells_line_refined and follows the WCVT approach.

N.	Model name	Grid type	Number of grid blocks	Top area grid block average (m^2)
1	01_structured	Structured	100	2500.00
2	02_Voronoi	Unstructured	100	2500.00
3	03_Quadtree_wells_refined	Unstructured	14902	16.78
4	04_Voronoi_wells_refined	Unstructured	14902	16.78
5	05_Quadtree_wells_line_refined	Unstructured	41419	6.04
6	06_Voronoi_wells_line_refined	Unstructured	41419	6.04

Table 4 – geometric characteristics of grids.

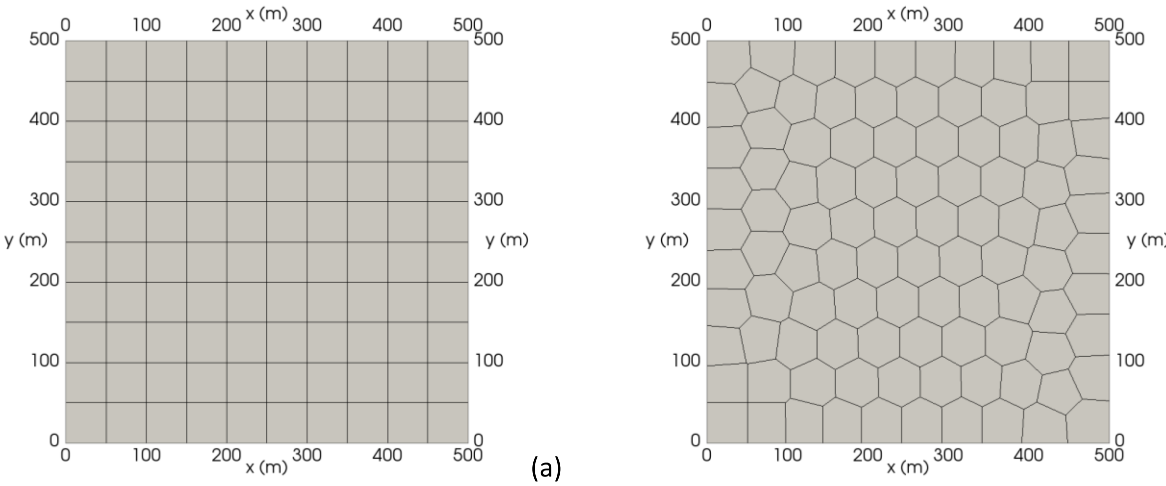

(a) (b)

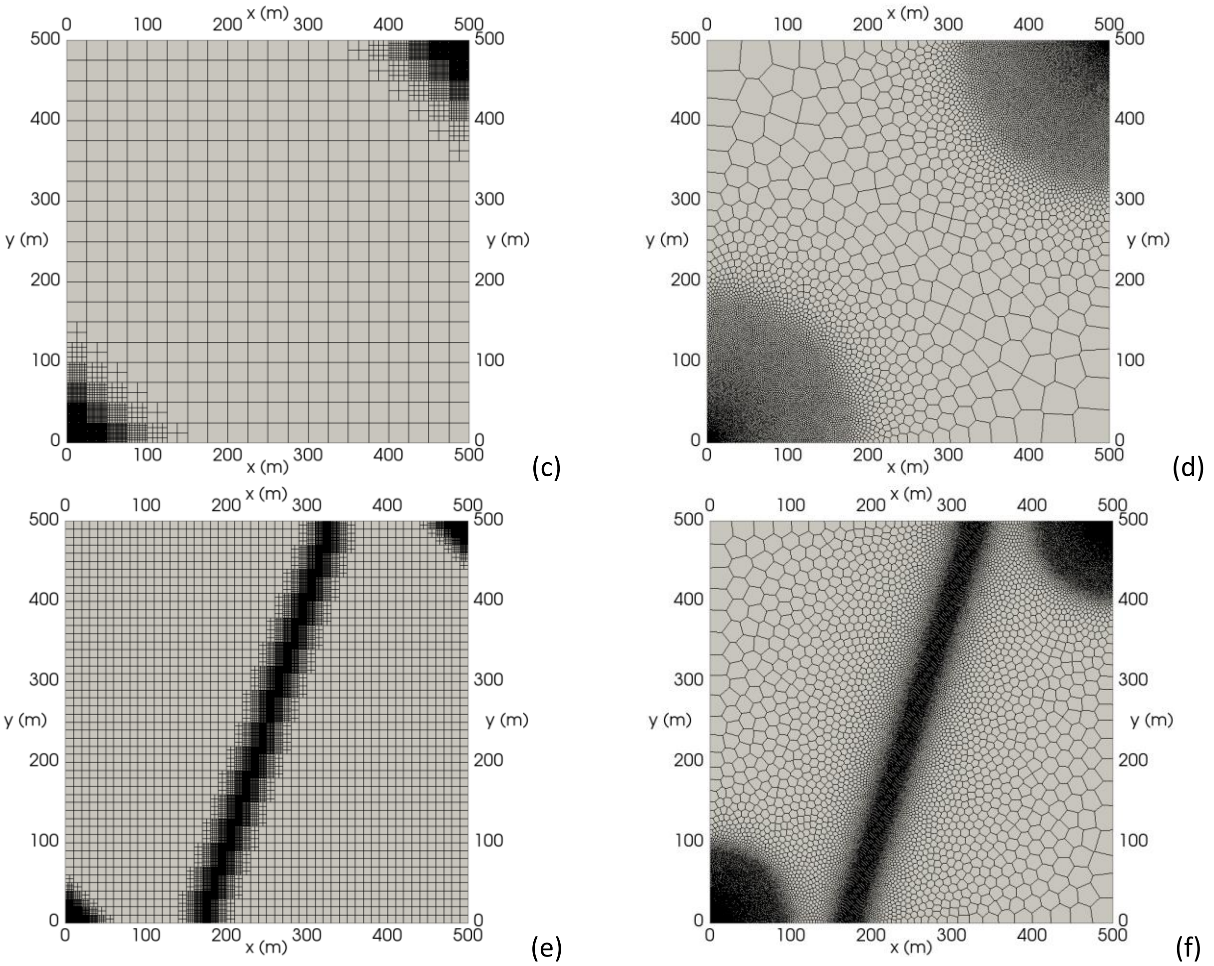

Figure 6– The discretization used for the different grids: (a) 01_structured; (b) 02_Voronoi; (c) 03_Quadtree_wells_refined; (d) Voronoi_wells_refined_C; (e) Quadtree_well_line_refined; (f) Voronoi_well_line_refined.

The computed dynamic evolution of the hydraulic head (pressure) has been computed considering an injection well with a volumetric rate of 1.0 m^3/s located at (0.01, 0.01) and a production well with a volumetric rate of -1.0 m^3/s located at the point (499.9, 499.9).

3 Results and Discussion

3.1.1 Case A: the 2D Darcy flow problem

The analytical solution of the presented problem is represented by the formula[2]:

$$h = 1 - \frac{1}{600}(x - 50)$$

Where h=hydraulic head (m), and x is the abscissa of the point, with $x \in (50.0; 650.0)$.

Figure 7 and Table 5 report the deviations of the simulation results computed on the three numerical models with respect to the analytical solutions.

[2] https://modflow6-examples.readthedocs.io/en/master/_examples/ex-gwf-u1gwfgwf.html [Last accessed 2022-09-15]

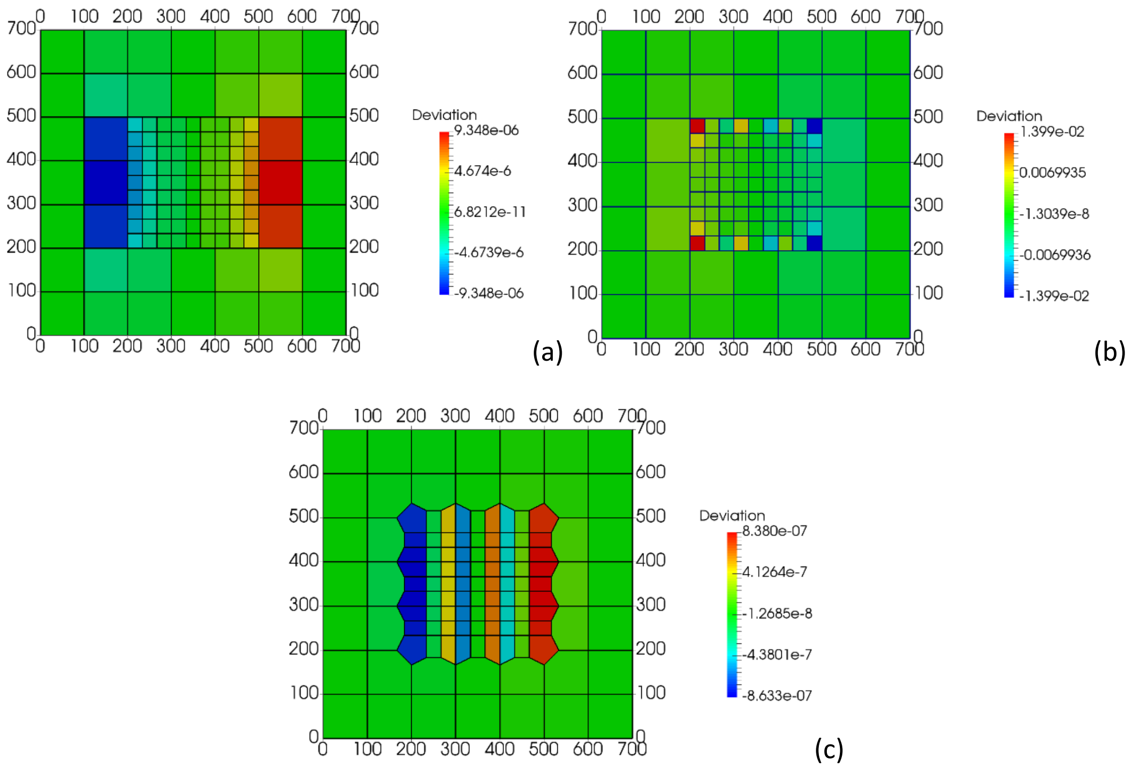

Figure 7– Deviations of the hydraulic head (in meters) computed with numerical simulations from those evaluated with the analytical solutions. (a) nested grid with GNC; (b) nested grid without GNC; (c) Voronoi grid.

Grid name	Deviation range (m)
01_Darcy_quadtree	[-9.348E-6, 9.348E-6]
02_Darcy_quadtree_NO_GNC	[-1.399E-2, 1.399E-2]
03_Darcy_Voronoi	[-8.380E-7, 8.380E-7]

Table 5 – Range of the deviations for the Darcy problem case study.

The deviations of the analytical and the numerical solutions of hydraulic head value using different grids are always in good agreement. The use of the GNC correction (01_Darcy_quadtree grid) allows reduction of the deviation by four orders of magnitude (see Table 5) with respect to the no-GNC grid (02_Darcy_quadtree_NO_GNC). The Voronoi grid shows a deviation very similar to the quadtree grid, with a slight improvement in accuracy (see Table 5 and Figure 7).

3.1.2 Case B: The 2D five-spot problem

The plots of the deviation between analytical and numerical head computations with MODFLOW 6 (6.0.4 version), as a function of the distance between the simulated block node and the well, are shown in Figure 8.

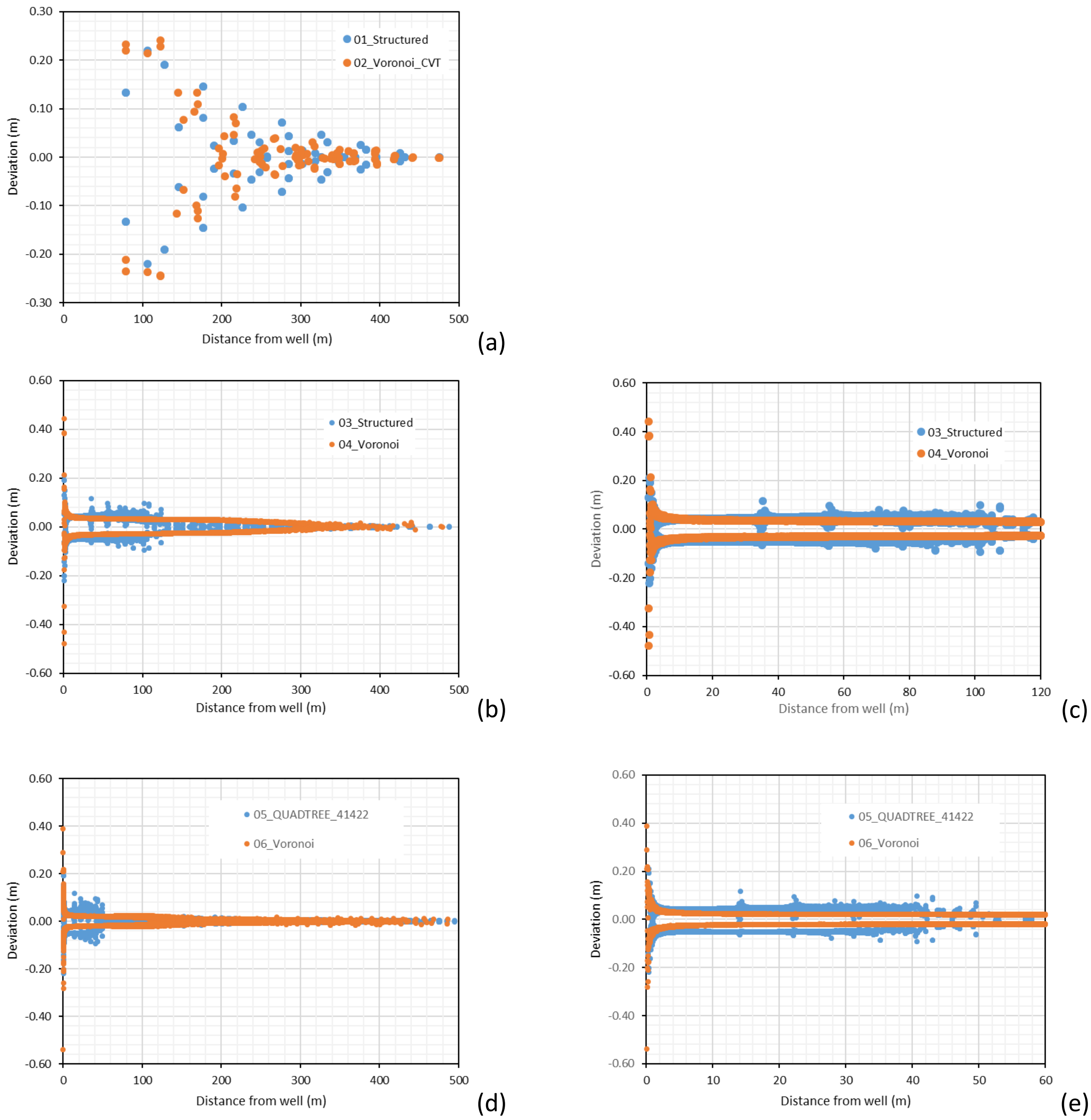

Figure 8 – (a) deviation comparison between the structured and unstructured Voronoi grids; (b) deviation comparison between the 03_quadtree and 04_voronoi grids, with well refinement; (c) the same as (b) with a zoom near the well zones; (d) deviation comparison between the grid 05_quadtree and 06_voronoi grid; (e) the same as (d) with a zoom near the well zones.

The heads computed on the first two grids (Figure 8.a) show a very similar behaviour, and the deviations from the analytical solution are almost identical. Note that in the Voronoi grid, the 3 blocks near the well sites have the same coordinates as the structured grid blocks. For the blocks located near the wells, it is possible to observe a marked difference of the Voronoi grid node position with respect to the quadtree grid blocks (distance from 70 up to 120 m). The difference is reduced at greater distances. It is worth mentioning that the physical system cannot be exactly replicated by the numerical model. So, for example, because of the finite dimension of the grid blocks, the wells cannot be located at coordinate (0.0,0.0) and (500.0,500.00), but in this simple case, they are located inevitably at (50.0, 50.0) and (450.0,450.0), respectively.

For the locally refined grids near the wells (03_quadtree and 04_Voronoi grids), the grid blocks representing the wells and the surrounding three blocks have the same coordinates. From the points plotted in Figure 8.b and Figure 8.c, it is possible to observe a similar behaviour as that observed in the previous comparison: the deviations of the Voronoi grid are higher near the wells (ca. in the first 5 meters), they are lower from 5 to 120 meters, and they are slightly higher for the longer distances.

For the last two grids, the 05_quadtree and the 06_Voronoi, we observe a very similar behaviour as in the previous two cases.

The spatial distributions of the deviations (deviation maps) with respect to the analytical solutions at the end of the simulation are shown in Figure 9.

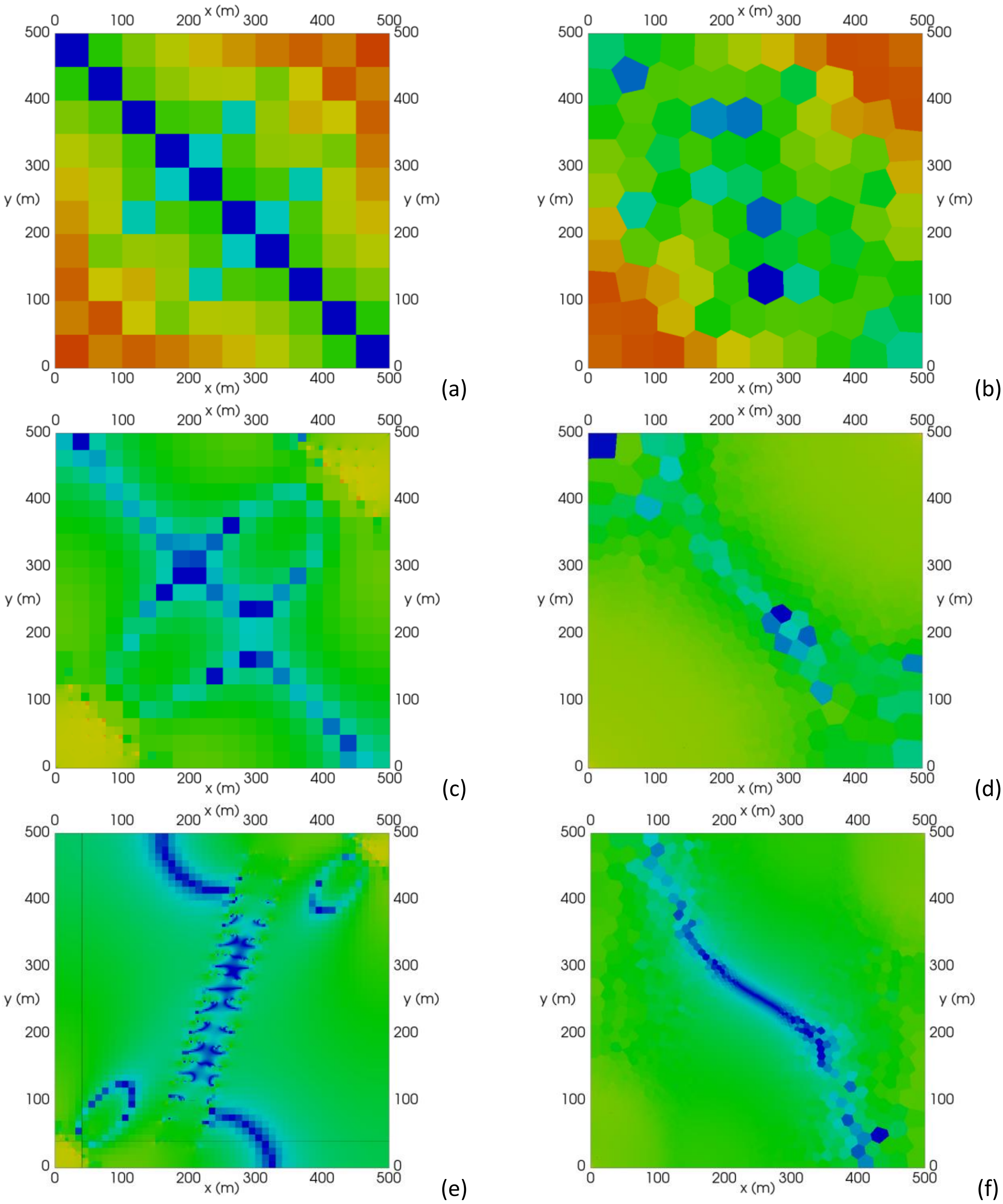

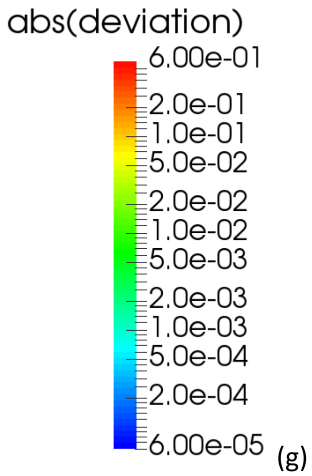

Figure 9 – Deviation grid maps. (a) 01_structured; (b) 02_Voronoi; (c) 03_quadtree; (d) 04_voronoi; (e) 05_quadtree; (f) 06_voronoi; (g) colour scale.

The deviation maps shown in Figure 9 (note that the colours refer to the absolute value of the deviation and they are in logarithmic scale) denotes a higher deviation related, in general, to the proximity to the well nodes, as already highlighted by the graphs in Figure 8. The quadtree grids (Figure 9.c and Figure 9.b) reveals higher (and lower) deviations near the blocks where the block size changes (due to the quadtree refinement), due to the ghost node correction operated by MODFLOW to reduce the error introduced when using non-conformal orthogonal grids. Conversely, the Voronoi grids do not suffer from the grid change resolution.

The deviation range (lower and upper values), average, and variance are shown in Table 6.

Grid name	Deviation range (m)	Average (m)	Variance (m^2)	Std_variance (m)
01_10x10_Structured	[-0.22, 0.22]	0.00000	0.00543	0.074
02_10x10_CVT_VORONOI	[-0.24, 0.24]	0.00013	0.00709	0.084
03_QUADTREE_14902_WELLS_REF	[-0.22, 0.21]	-0.00477	0.00218	0.047
04_VORONOI_well_refined	[-0.44, 0.44]	0.00144	0.00104	0.032
05_QUADTREE_41422_WELLS	[-0.22, 0.21]	-0.00173	0.00079	0.028
06_VORONOI_WELLS_A	[-0.54, 0.39]	0.00013	0.00028	0.017

Table 6 – Statistical values of the deviation for the six examined grids.

In general, results show that the deviation observed in the six grids are very close to the analytical solution used as a reference, and therefore that all grids can be used to correctly reproduce the five-spot problem. The Voronoi grid exhibits higher isolated deviation errors near the wells, while the deviation average in the whole domain is lower, as well as the standard deviation is lower for the Voronoi grids. The use of the Voronoi grids allows a local grid refinement where model features require a finer resolution without introducing ghost node corrections and reduce the deviation between the analytical and numerical model results near LGR zones.

The computational time for the presented problem is shown in Table 7. The simulation has been performed using a PC equipped with a Intel(R) Core(TM) i7-6700HQ, CPU @ 2.60GHz, 16 MB of RAM.

Grid name	Total Computation time (s)
01_10x10_Structured	4.046
02_10x10_CVT_VORONOI	3.876
03_QUADTREE_14902_WELLS_REF	18.963

04_VORONOI_well_refined	10.466
05_QUADTREE_41422_WELLS	48.351
06_VORONOI_WELLS_A	17.644

Table 7 – Computational time for the different grids.

The computation time of the unstructured Voronoi grids is lower than the LGR grids. The gap increases by increasing the size of the grid.

4 Conclusions

VORO2MESH and TOUGH2Viewer provides a flexible tool for the calculation of VORONOI grids, grid editing, and results visualization for MODFLOW numerical models. To the best knowledge of the authors, there are not dedicated free and open source software for VORONOI grid generation for MODFLOW published in the scientific literature. Among the others capabilities, it is worth to mention the capability of TOUGH2Viewer of exporting the numerical results in a file format for PARAVIEW, one of the most powerful visualization tools available in the literature, for scientific applications.

The validity of the two tools has been demonstrated on two case studies. The comparison of numerical simulation results with analytical solutions strongly highlighted the usefulness of these tools in simulations. In the local grid refinements with Voronoi grids, which implicitly satisfy the orthogonality requirement, there is a small lower loss of accuracy with respect to the analytical solution than when the refinements are made on square grids that adopt the ghost node corrections.

Due to its utility and simplicity of use, it is expected that VORO2MESH and TOUGH2Viewer will assist hydrogeologists and environmental scientists in using MODFLOW simulator with VORONOI grids, improving the performance of the simulation tasks, including results analysis and visualization.

Future work will include the possibility of VORO2MESH to produce 2.5D grids for MODFLOW.

VORO2MESH and TOUGH2Viewer can be freely used and downloaded from:

https://site.unibo.it/softwaredicam/en/software/voro2mesh and
https://site.unibo.it/softwaredicam/en/software/tough2viewer.

5 References

Ahrens, J., Geveci, B., Law, C., 2005. ParaView: An end-user tool for large-data visualization, Visualization Handbook. https://doi.org/10.1016/B978-012387582-2/50038-1

Aliyari, F., Bailey, R.T., Tasdighi, A., Dozier, A., Arabi, M., Zeiler, K., 2019. Coupled SWAT-MODFLOW model for large-scale mixed agro-urban river basins. Environ. Model. Softw. 115, 200–210. https://doi.org/https://doi.org/10.1016/j.envsoft.2019.02.014

Bailey, R.T., Park, S., Bieger, K., Arnold, J.G., Allen, P.M., 2020. Enhancing SWAT+ simulation of groundwater flow and groundwater-surface water interactions using MODFLOW routines. Environ. Model. Softw. 126, 104660. https://doi.org/https://doi.org/10.1016/j.envsoft.2020.104660

Bakker, M., Post, V.., Langevin, C.D., Hughes, J.D., White, J.T., Starn, J.J., Fienen, M.N., 2016. Scripting MODFLOW model development using Python and FloPy. Groundwater 54, 733–739.

Barber, C.B., Dobkin, D.P., Dobkin, D.P., Huhdanpaa, H., 1996. The Quickhull Algorithm for Convex Hulls. ACM Trans. Math. Softw. 22, 469–483. https://doi.org/10.1145/235815.235821

Bear, J.J., Cheng, H.-D.A., 2010. Numerical Models and Computer Codes, in: Modeling Groundwater Flow and Contaminant Transport. Springer Netherlands, Dordrecht. https://doi.org/10.1007/978-1-4020-6682-5_8

Bedekar, V., Morway, E.D., Langevin, C.D., Tonkin, M.J., 2016. MT3D-USGS version 1: A U.S. Geological Survey release of MT3DMS updated with new and expanded transport capabilities for use with MODFLOW, Techniques and Methods. Reston, VA. https://doi.org/10.3133/tm6A53

Bittner, D., Rychlik, A., Klöffel, T., Leuteritz, A., Disse, M., Chiogna, G., 2020. A GIS-based model for simulating the hydrological effects of land use changes on karst systems – The integration of the LuKARS model into FREEWAT. Environ. Model. Softw. 127, 104682. https://doi.org/https://doi.org/10.1016/j.envsoft.2020.104682

Bonduà, S., Battistelli, A., Berry, P., Bortolotti, V., Consonni, A., Cormio, C., Geloni, C., Vasini, E.M., 2017. 3D Voronoi grid dedicated software for modeling gas migration in deep layered sedimentary formations with TOUGH2-TMGAS. Comput. Geosci. 108, 50–55. https://doi.org/https://doi.org/10.1016/j.cageo.2017.03.008

Bondua, S., Berry, P., Bortolotti, V., Cormio, C., 2012. TOUGH2Viewer: A post-processing tool for interactive 3D visualization of locally refined unstructured grids for TOUGH2. Comput. Geosci. 46, 107–118. https://doi.org/10.1016/j.cageo.2012.04.008

Bonduà, S., Bortolotti, V., 2020. TOUGH2Viewer 2.0: A multiplatform tool for fully 3D Voronoi TOUGH grids. SoftwareX 12, 100596. https://doi.org/https://doi.org/10.1016/j.softx.2020.100596

Chen, Y., Marek, G.W., Marek, T.H., Brauer, D.K., Srinivasan, R., 2018. Improving SWAT auto-irrigation functions for simulating agricultural irrigation management using long-term lysimeter field data. Environ. Model. Softw. 99, 25–38. https://doi.org/https://doi.org/10.1016/j.envsoft.2017.09.013

Du, Q., Faber, V., Gunzburger, M., 1999. Centroidal Voronoi tessellations: Applications and algorithms. SIAM Rev. 41, 637–676.

Elsayed, S.M., Oumeraci, H., 2018. Modelling and mitigation of storm-induced saltwater intrusion: Improvement of the resilience of coastal aquifers against marine floods by subsurface drainage. Environ. Model. Softw. 100, 252–277. https://doi.org/https://doi.org/10.1016/j.envsoft.2017.11.030

Esfahani, S.G., Valocchi, A.J., Werth, C.J., 2021. Using MODFLOW and RT3D to simulate diffusion and reaction without discretizing low permeability zones. J. Contam. Hydrol. 239, 103777. https://doi.org/https://doi.org/10.1016/j.jconhyd.2021.103777

Gardner, M.A., Morton, C.G., Huntington, J.L., Niswonger, R.G., Henson, W.R., 2018. Input data processing tools for the integrated hydrologic model GSFLOW. Environ. Model. Softw. 109, 41–53. https://doi.org/https://doi.org/10.1016/j.envsoft.2018.07.020

González, R.E., 2016. PARAVT: Parallel Voronoi tessellation code. Astron. Comput. 17, 80–85. https://doi.org/10.1016/j.ascom.2016.06.003

Guzman, J.A., Moriasi, D.N., Gowda, P.H., Steiner, J.L., Starks, P.J., Arnold, J.G., Srinivasan, R., 2015. A model integration framework for linking SWAT and MODFLOW. Environ. Model. Softw. 73, 103–116. https://doi.org/https://doi.org/10.1016/j.envsoft.2015.08.011

Harbaugh, A.W., 2005. MODFLOW-2005, the U.S. Geological Survey modular ground-water model-The Ground-Water Flow Process. MODFLOW-2005, U.S. Geol. Surv. Modul. Ground-water Model - Ground-water Flow Process.

Hariharan, V., Uma Shankar, M., 2017. A review of visual modflow applications in groundwater modelling, in: IOP Conference Series: Materials Science and Engineering. Institute of Physics Publishing. https://doi.org/10.1088/1757-899X/263/3/032025

Hughes, J.D., Langevin, C.D., Banta, E.R., 2017. Documentation for the MODFLOW 6 framework, Techniques and Methods. Reston, VA. https://doi.org/10.3133/tm6A57

Inaba, M., Katoh, N., Imai, H., 1994. Applications of weighted voronoi diagrams and randomization to variance-based k-clustering, in: Proceedings of the Annual Symposium on Computational Geometry. pp. 332–339. https://doi.org/10.1145/177424.178042

Langevin, C.D., Hughes, J.D., Banta, E.R., Niswonger, R.G., Panday, S., Provost, A.M., 2017. Documentation for the MODFLOW 6 Groundwater Flow Model, Techniques and Methods. Reston, VA. https://doi.org/10.3133/tm6A55

Maleki Tirabadi, M.S., Banihabib, M.E., Randhir, T.O., 2021. SWAT-S: A SWAT-salinity module for watershed-scale modeling of natural salinity. Environ. Model. Softw. 135, 104906. https://doi.org/https://doi.org/10.1016/j.envsoft.2020.104906

Mehl, S.W., Hill, M.C., 2013. MODFLOW-LGR-Documentation of Ghost Node Local Grid Refinement (LGR2) for Multiple Areas and the Boundary Flow and Head (BFH2) Package. US Geol. Surv. Tech. Methods 6-A44.

Panday, S., Langevin, C.D., 2012. Improving sub-grid scale accuracy of boundary features in regional finite-difference models. Adv. Water Resour. 41, 65–75. https://doi.org/10.1016/j.advwatres.2012.02.011

Panday, S., Langevin, C.D., Niswonger, R.G., Ibaraki, M., Hughes, J.D., 2013. MODFLOW–USG version 1: An unstructured grid version of MODFLOW for simulating groundwater flow and tightly coupled processes using a control volume finite-difference formulation, Techniques and Methods. Reston, VA. https://doi.org/10.3133/tm6A45

Park, S., Nielsen, A., Bailey, R.T., Trolle, D., Bieger, K., 2019. A QGIS-based graphical user interface for application and evaluation of SWAT-MODFLOW models. Environ. Model. Softw. 111, 493–497. https://doi.org/https://doi.org/10.1016/j.envsoft.2018.10.017

Provost, A.M., Langevin, C.D., Hughes, J.D., 2017. Documentation for the “XT3D” option in the Node Property Flow (NPF) Package of MODFLOW 6. Tech. Methods. https://doi.org/10.3133/TM6A56

Pruess, K., Oldenburg, C.M., Moridis, G.J., 1999. TOUGH2 User’s Guide Version 2.

Rossetto, R., Filippis, G. De, Triana, F., Ghetta, M., Borsi, I., Schmid, W., 2019. Software tools for management of conjunctive use of surface- and ground-water in the rural environment: integration of the Farm Process and the Crop Growth Module in the FREEWAT platform. Agric. Water Manag. 223, 105717. https://doi.org/https://doi.org/10.1016/j.agwat.2019.105717

Rumbaugh, J.O., Rumbaugh, D.B., 2011. Guide to Using Groundwater Vistas, Version 6, Environmental Simulations. Inc., Reinholds, Pennsylvania, USA.

Rycroft, C.H., 2009. VORO++: A three-dimensional Voronoi cell library in C++. Chaos 19. https://doi.org/10.1063/1.3215722

Si, H., 2015. TetGen, a Delaunay-Based Quality Tetrahedral Mesh Generator. ACM Trans. Math. Softw. 41, 11:1--11:36. https://doi.org/10.1145/2629697

The CGAL Project, 2018. User and Reference Manual, 4.13. ed. CGAL Editorial Board.

Theis, C. V, 1935. The relation between the lowering of the Piezometric surface and the rate and duration of discharge of a well using ground-water storage. Trans. Am. Geophys. Union 16, 519–524. https://doi.org/10.1029/TR016i002p00519

Tian, Y., Zheng, Y., Han, F., Zheng, C., Li, X., 2018. A comprehensive graphical modeling platform designed for integrated hydrological simulation. Environ. Model. Softw. 108, 154–173. https://doi.org/https://doi.org/10.1016/j.envsoft.2018.08.011

Wei, X., Bailey, R.T., Records, R.M., Wible, T.C., Arabi, M., 2019. Comprehensive simulation of nitrate transport in coupled surface-subsurface hydrologic systems using the linked SWAT-MODFLOW-RT3D model. Environ. Model. Softw. 122, 104242. https://doi.org/https://doi.org/10.1016/j.envsoft.2018.06.012

Winston, R.B., 2009. ModelMuse: A Graphical User Interface for MODFLOW-2005 and PHAST. U.S. Geol. Surv. Tech. Methods 6-A29.

6 Appendix A

Example of the output files produced by VORO2MESH for the grid in Figure 4.b.

- flow.disu

```
# Unstructured discretization file for MODFLOW-USG
begin options
  LENGTH_UNITS meters
end options

begin dimensions
  nodes 121
  nja 609
end dimensions

BEGIN GRIDDATA
  top
    open/close 'flow.disu.top.dat'   IPRN 0
  bot
    open/close 'flow.disu.bottom.dat'   IPRN 0
  area
    open/close 'flow.disu.area.dat' FACTOR  1.0
END GRIDDATA

begin connectiondata
  ihc
    open/close 'flow.disu.ihc.dat'   IPRN 0
  iac
    open/close 'flow.disu.iac.dat'   IPRN 0
  ja
    open/close 'flow.disu.ja.dat' FACTOR  1
  cl12
    open/close 'flow.disu.cl12.dat'  FACTOR  1.0  IPRN 0
  hwva
    open/close 'flow.disu.hwva.dat' FACTOR  1.0  IPRN 0
end connectiondata
```

- flow.disu.area.dat

```
      10000       10000       10000       10000       10000
      10000       10000       10000     9444.44     7777.78
    7777.78     7777.78     9444.44       10000       10000
    7777.78     7777.78       10000       10000     7777.78
    7777.78       10000       10000     7777.78     7777.78
      10000       10000     9444.44     7777.78     7777.78
    7777.78     9444.44       10000       10000       10000
      10000       10000       10000       10000       10000
    3333.33     1666.67     1944.44     1944.44     1666.67
    1944.44     1944.44     1666.67     3333.33     1666.67
    1111.11     1111.11     1111.11     1111.11     1111.11
    1111.11     1111.11     1666.67     1944.44     1111.11
```

```
      1111.11      1111.11      1111.11      1111.11      1111.11
      1111.11      1944.44      1944.44      1111.11      1111.11
      1111.11      1111.11      1111.11      1111.11      1111.11
      1944.44      1666.67      1111.11      1111.11      1111.11
      1111.11      1111.11      1111.11      1111.11      1666.67
      1944.44      1111.11      1111.11      1111.11      1111.11
      1111.11      1111.11      1111.11      1944.44      1944.44
      1111.11      1111.11      1111.11      1111.11      1111.11
      1111.11      1111.11      1944.44      1666.67      1111.11
      1111.11      1111.11      1111.11      1111.11      1111.11
      1111.11      1666.67      3333.33      1666.67      1944.44
      1944.44      1666.67      1944.44      1944.44      1666.67
      3333.33
```

- flow.disu.bottom.dat

```
         -100         -100         -100         -100         -100
         -100         -100         -100         -100         -100
         -100         -100         -100         -100         -100
         -100         -100         -100         -100         -100
         -100         -100         -100         -100         -100
         -100         -100         -100         -100         -100
         -100         -100         -100         -100         -100
         -100         -100         -100         -100         -100
         -100         -100         -100         -100         -100
         -100         -100         -100         -100         -100
         -100         -100         -100         -100         -100
         -100         -100         -100         -100         -100
         -100         -100         -100         -100         -100
         -100         -100         -100         -100         -100
         -100         -100         -100         -100         -100
         -100         -100         -100         -100         -100
         -100         -100         -100         -100         -100
         -100         -100         -100         -100         -100
         -100         -100         -100         -100         -100
         -100         -100         -100         -100         -100
         -100         -100         -100         -100         -100
         -100         -100         -100         -100         -100
         -100         -100         -100         -100         -100
         -100         -100         -100         -100         -100
         -100
```

- flow.disu.top.dat

```
            0            0            0            0            0
            0            0            0            0            0
            0            0            0            0            0
            0            0            0            0            0
            0            0            0            0            0
            0            0            0            0            0
            0            0            0            0            0
            0            0            0            0            0
            0            0            0            0            0
            0            0            0            0 -7.10543e-15
            0            0 -7.10543e-15            0            0
            0            0            0            0            0
            0            0            0            0            0
            0            0 -7.10543e-15 -7.10543e-15            0
            0            0            0            0  7.10543e-15
 -7.10543e-15  7.10543e-15            0            0            0
            0            0 -7.10543e-15            0  7.10543e-15
            0            0            0 -7.10543e-15            0
  7.10543e-15            0 -7.10543e-15            0            0
            0            0            0            0            0
            0            0            0            0            0
            0 -1.42109e-14            0            0            0
            0            0            0            0            0
            0            0            0            0            0
  7.10543e-15
```

- flow.disu.cl12.dat

0	50	50	0	50
50	50	0	50	50
50	0	50	50	50
0	50	50	50	0
50	50	50	0	50
50	0	50	50	50
0	50	50	50	50
47.1405	0	50	50	50
37.2678	33.3333	37.2678	0	50
50	50	37.2678	33.3333	37.2678
0	50	50	50	37.2678
33.3333	37.2678	0	50	50
50	50	47.1405	0	50
50	50	0	50	50
50	0	50	50	50
37.2678	33.3333	37.2678	0	50
50	50	37.2678	33.3333	37.2678
0	50	50	50	0
50	50	50	0	50
50	50	37.2678	33.3333	37.2678
0	50	50	50	37.2678
33.3333	37.2678	0	50	50
50	0	50	50	50
0	50	50	50	37.2678
33.3333	37.2678	0	50	50
50	37.2678	33.3333	37.2678	0
50	50	50	0	50
50	50	0	50	50
50	50	47.1405	0	50
50	50	37.2678	33.3333	37.2678
0	50	50	50	37.2678
33.3333	37.2678	0	50	50
50	37.2678	33.3333	37.2678	0
50	50	50	50	47.1405
0	50	50	50	0
50	50	0	50	50
50	0	50	50	50
0	50	50	50	0
50	50	50	0	50
50	50	0	50	50
0	47.1405	37.2678	37.2678	16.6667
16.6667	0	33.3333	16.6667	16.6667
16.6667	0	37.2678	16.6667	16.6667
16.6667	0	37.2678	16.6667	16.6667
16.6667	0	33.3333	16.6667	16.6667
16.6667	0	37.2678	16.6667	16.6667
16.6667	0	37.2678	16.6667	16.6667
16.6667	0	33.3333	16.6667	16.6667
16.6667	0	37.2678	47.1405	37.2678
16.6667	16.6667	0	33.3333	16.6667
16.6667	16.6667	0	16.6667	16.6667
16.6667	16.6667	0	16.6667	16.6667
16.6667	16.6667	0	16.6667	16.6667
16.6667	16.6667	0	16.6667	16.6667
16.6667	16.6667	0	16.6667	16.6667
16.6667	16.6667	0	16.6667	16.6667
16.6667	16.6667	0	16.6667	16.6667
16.6667	16.6667	0	33.3333	16.6667
16.6667	16.6667	0	37.2678	16.6667
16.6667	16.6667	0	16.6667	16.6667
16.6667	16.6667	0	16.6667	16.6667
16.6667	16.6667	0	16.6667	16.6667
16.6667	16.6667	0	16.6667	16.6667
16.6667	16.6667	0	16.6667	16.6667
16.6667	16.6667	0	16.6667	16.6667
16.6667	16.6667	0	16.6667	16.6667
16.6667	16.6667	0	37.2678	16.6667
16.6667	16.6667	0	37.2678	16.6667
16.6667	16.6667	0	16.6667	16.6667
16.6667	16.6667	0	16.6667	16.6667
16.6667	16.6667	0	16.6667	16.6667
16.6667	16.6667	0	16.6667	16.6667
16.6667	16.6667	0	16.6667	16.6667
16.6667	16.6667	0	16.6667	16.6667
16.6667	16.6667	0	16.6667	16.6667
16.6667	16.6667	0	37.2678	16.6667
16.6667	16.6667	0	33.3333	16.6667
16.6667	16.6667	0	16.6667	16.6667

16.6667	16.6667	0	16.6667	16.6667
16.6667	16.6667	0	16.6667	16.6667
16.6667	16.6667	0	16.6667	16.6667
16.6667	16.6667	0	16.6667	16.6667
16.6667	16.6667	0	16.6667	16.6667
16.6667	16.6667	0	16.6667	16.6667
16.6667	16.6667	0	33.3333	16.6667
16.6667	16.6667	0	37.2678	16.6667
16.6667	16.6667	0	16.6667	16.6667
16.6667	16.6667	0	16.6667	16.6667
16.6667	16.6667	0	16.6667	16.6667
16.6667	16.6667	0	16.6667	16.6667
16.6667	16.6667	0	16.6667	16.6667
16.6667	16.6667	0	16.6667	16.6667
16.6667	16.6667	0	16.6667	16.6667
16.6667	16.6667	0	37.2678	16.6667
16.6667	16.6667	0	37.2678	16.6667
16.6667	16.6667	0	16.6667	16.6667
16.6667	16.6667	0	16.6667	16.6667
16.6667	16.6667	0	16.6667	16.6667
16.6667	16.6667	0	16.6667	16.6667
16.6667	16.6667	0	16.6667	16.6667
16.6667	16.6667	0	16.6667	16.6667
16.6667	16.6667	0	16.6667	16.6667
16.6667	16.6667	0	37.2678	16.6667
16.6667	16.6667	0	33.3333	16.6667
16.6667	16.6667	0	16.6667	16.6667
16.6667	16.6667	0	16.6667	16.6667
16.6667	16.6667	0	16.6667	16.6667
16.6667	16.6667	0	16.6667	16.6667
16.6667	16.6667	0	16.6667	16.6667
16.6667	16.6667	0	16.6667	16.6667
16.6667	16.6667	0	16.6667	16.6667
16.6667	16.6667	0	33.3333	16.6667
16.6667	16.6667	0	37.2678	47.1405
37.2678	16.6667	16.6667	0	33.3333
16.6667	16.6667	16.6667	0	37.2678
16.6667	16.6667	16.6667	0	37.2678
16.6667	16.6667	16.6667	0	33.3333
16.6667	16.6667	16.6667	0	37.2678
16.6667	16.6667	16.6667	0	37.2678
16.6667	16.6667	16.6667	0	33.3333
16.6667	16.6667	16.6667	0	37.2678
37.2678	47.1405	16.6667	16.6667	

- flow.disu.hwva.dat

0	100	100				
0	100	100	100			
0	100	100	100			
0	100	100	100			
0	100	100	100			
0	100	100	100			
0	100	100				
0	100	100	100			
0	100	100	66.6667	66.6667	47.1405	
0	100	66.6667	66.6667	37.2678	33.3333	37.2678
0	100	66.6667	66.6667	37.2678	33.3333	37.2678
0	100	66.6667	66.6667	37.2678	33.3333	37.2678
0	100	66.6667	100	66.6667	47.1405	
0	100	100	100			
0	100	100	100			
0	66.6667	100	66.6667	37.2678	33.3333	37.2678
0	66.6667	100	66.6667	37.2678	33.3333	37.2678
0	100	100	100			
0	100	100	100			
0	66.6667	100	66.6667	37.2678	33.3333	37.2678
0	66.6667	100	66.6667	37.2678	33.3333	37.2678
0	100	100	100			
0	100	100	100			
0	66.6667	100	66.6667	37.2678	33.3333	37.2678
0	66.6667	100	66.6667	37.2678	33.3333	37.2678
0	100	100	100			
0	100	100	100			
0	66.6667	100	66.6667	100	47.1405	

0	66.6667	66.6667	100	37.2678	33.3333	37.2678
0	66.6667	66.6667	100	37.2678	33.3333	37.2678
0	66.6667	66.6667	100	37.2678	33.3333	37.2678
0	66.6667	66.6667	100	100	47.1405	
0	100	100	100			
0	100	100				
0	100	100	100			
0	100	100	100			
0	100	100	100			
0	100	100	100			
0	100	100	100			
0	100	100				
0	47.1405	37.2678	37.2678	50	50	
0	33.3333	50	50	33.3333		
0	37.2678	50	66.6667	33.3333		
0	37.2678	66.6667	50	33.3333		
0	33.3333	50	50	33.3333		
0	37.2678	50	66.6667	33.3333		
0	37.2678	66.6667	50	33.3333		
0	33.3333	50	50	33.3333		
0	37.2678	47.1405	37.2678	50	50	
0	33.3333	50	33.3333	50		
0	33.3333	33.3333	33.3333	33.3333		
0	33.3333	33.3333	33.3333	33.3333		
0	33.3333	33.3333	33.3333	33.3333		
0	33.3333	33.3333	33.3333	33.3333		
0	33.3333	33.3333	33.3333	33.3333		
0	33.3333	33.3333	33.3333	33.3333		
0	33.3333	33.3333	33.3333	33.3333		
0	33.3333	50	33.3333	50		
0	37.2678	50	33.3333	66.6667		
0	33.3333	33.3333	33.3333	33.3333		
0	33.3333	33.3333	33.3333	33.3333		
0	33.3333	33.3333	33.3333	33.3333		
0	33.3333	33.3333	33.3333	33.3333		
0	33.3333	33.3333	33.3333	33.3333		
0	33.3333	33.3333	33.3333	33.3333		
0	33.3333	33.3333	33.3333	33.3333		
0	37.2678	50	33.3333	66.6667		
0	37.2678	66.6667	33.3333	50		
0	33.3333	33.3333	33.3333	33.3333		
0	33.3333	33.3333	33.3333	33.3333		
0	33.3333	33.3333	33.3333	33.3333		
0	33.3333	33.3333	33.3333	33.3333		
0	33.3333	33.3333	33.3333	33.3333		
0	33.3333	33.3333	33.3333	33.3333		
0	33.3333	33.3333	33.3333	33.3333		
0	37.2678	66.6667	33.3333	50		
0	33.3333	50	33.3333	50		
0	33.3333	33.3333	33.3333	33.3333		
0	33.3333	33.3333	33.3333	33.3333		
0	33.3333	33.3333	33.3333	33.3333		
0	33.3333	33.3333	33.3333	33.3333		
0	33.3333	33.3333	33.3333	33.3333		
0	33.3333	33.3333	33.3333	33.3333		
0	33.3333	33.3333	33.3333	33.3333		
0	33.3333	50	33.3333	50		
0	37.2678	50	33.3333	66.6667		
0	33.3333	33.3333	33.3333	33.3333		
0	33.3333	33.3333	33.3333	33.3333		
0	33.3333	33.3333	33.3333	33.3333		
0	33.3333	33.3333	33.3333	33.3333		
0	33.3333	33.3333	33.3333	33.3333		
0	33.3333	33.3333	33.3333	33.3333		
0	33.3333	33.3333	33.3333	33.3333		
0	37.2678	50	33.3333	66.6667		
0	37.2678	66.6667	33.3333	50		
0	33.3333	33.3333	33.3333	33.3333		
0	33.3333	33.3333	33.3333	33.3333		
0	33.3333	33.3333	33.3333	33.3333		
0	33.3333	33.3333	33.3333	33.3333		
0	33.3333	33.3333	33.3333	33.3333		
0	33.3333	33.3333	33.3333	33.3333		
0	33.3333	33.3333	33.3333	33.3333		
0	37.2678	66.6667	33.3333	50		
0	33.3333	50	33.3333	50		
0	33.3333	33.3333	33.3333	33.3333		
0	33.3333	33.3333	33.3333	33.3333		

```
         0      33.3333      33.3333      33.3333      33.3333
         0      33.3333      33.3333      33.3333      33.3333
         0      33.3333      33.3333      33.3333      33.3333
         0      33.3333      33.3333      33.3333      33.3333
         0      33.3333      33.3333      33.3333      33.3333
         0      33.3333           50      33.3333           50
         0      37.2678      47.1405      37.2678           50           50
         0      33.3333      33.3333           50           50
         0      37.2678      33.3333           50      66.6667
         0      37.2678      33.3333      66.6667           50
         0      33.3333      33.3333           50           50
         0      37.2678      33.3333           50      66.6667
         0      37.2678      33.3333      66.6667           50
         0      33.3333      33.3333           50           50
         0      37.2678      37.2678      47.1405           50           50
```

- flow.disu.ihc.dat:

```
         1            1            1            1            1
         1            1            1            1            1
         1            1            1            1            1
         1            1            1            1            1
         1            1            1            1            1
         1            1            1            1            1
         1            1            1            1            1
         1            1            1            1            1
         1            1            1            1            1
         1            1            1            1            1
         1            1            1            1            1
         1            1            1            1            1
         1            1            1            1            1
         1            1            1            1            1
         1            1            1            1            1
         1            1            1            1            1
         1            1            1            1            1
         1            1            1            1            1
         1            1            1            1            1
         1            1            1            1            1
         1            1            1            1            1
         1            1            1            1            1
         1            1            1            1            1
         1            1            1            1            1
         1            1            1            1            1
         1            1            1            1            1
         1            1            1            1            1
         1            1            1            1            1
         1            1            1            1            1
         1            1            1            1            1
         1            1            1            1            1
         1            1            1            1            1
         1            1            1            1            1
         1            1            1            1            1
         1            1            1            1            1
         1            1            1            1            1
         1            1            1            1            1
         1            1            1            1            1
         1            1            1            1            1
         1            1            1            1            1
         1            1            1            1            1
         1            1            1            1            1
         1            1            1            1            1
         1            1            1            1            1
         1            1            1            1            1
         1            1            1            1            1
         1            1            1            1            1
         1            1            1            1            1
         1            1            1            1            1
         1            1            1            1            1
         1            1            1            1            1
         1            1            1            1            1
         1            1            1            1            1
         1            1            1            1            1
         1            1            1            1            1
         1            1            1            1            1
         1            1            1            1            1
         1            1            1            1            1
         1            1            1            1            1
         1            1            1            1            1
```

```
1 1 1 1 1
1 1 1 1 1
1 1 1 1 1
1 1 1 1 1
1 1 1 1 1
1 1 1 1 1
1 1 1 1 1
1 1 1 1 1
1 1 1 1 1
1 1 1 1 1
1 1 1 1 1
1 1 1 1 1
1 1 1 1 1
1 1 1 1 1
1 1 1 1 1
1 1 1 1 1
1 1 1 1 1
1 1 1 1 1
1 1 1 1 1
1 1 1 1 1
1 1 1 1 1
1 1 1 1 1
1 1 1 1 1
1 1 1 1 1
1 1 1 1 1
1 1 1 1 1
1 1 1 1 1
1 1 1 1 1
1 1 1 1 1
1 1 1 1 1
1 1 1 1 1
1 1 1 1 1
1 1 1 1 1
1 1 1 1 1
1 1 1 1 1
1 1 1 1 1
1 1 1 1 1
1 1 1 1 1
1 1 1 1 1
1 1 1 1 1
1 1 1 1 1
1 1 1 1 1
1 1 1 1 1
1 1 1 1 1
1 1 1 1 1
1 1 1 1 1
1 1 1 1 1
1 1 1 1 1
1 1 1 1 1
1 1 1 1 1
1 1 1 1 1
1 1 1 1 1
1 1 1 1 1
1 1 1 1 1
1 1 1 1 1
1 1 1 1 1
1 1 1 1 1
1 1 1 1 1
1 1 1 1 1
1 1 1 1 1
1 1 1 1 1
1 1 1 1
```

- flow.disu.ja.dat

```
 1  2  8  2  1
 3  9  3  2  4
10  4  3  5 11
 5  4  6 12  6
 5  7 13  7  6
14  8  1  9 15
 9  2  8 10 16
41 10  3  9 11
41 42 43 11  4
10 12 44 45 46
12  5 11 13 47
48 49 13  6 12
14 17 49 14  7
```

13	18	15	8	16
19	16	9	15	20
41	50	59	17	13
18	21	49	58	67
18	14	17	22	19
15	20	23	20	16
19	24	68	77	86
21	17	22	25	76
85	94	22	18	21
26	23	19	24	27
24	20	23	28	95
104	113	25	21	26
32	103	112	121	26
22	25	33	27	23
28	34	28	24	27
29	35	113	29	28
30	36	113	114	115
30	29	31	37	116
117	118	31	30	32
38	119	120	121	32
25	31	33	39	121
33	26	32	40	34
27	35	35	28	34
36	36	29	35	37
37	30	36	38	38
31	37	39	39	32
38	40	40	33	39
41	9	10	16	42
50	42	10	41	43
51	43	10	42	44
52	44	11	43	45
53	45	11	44	46
54	46	11	45	47
55	47	12	46	48
56	48	12	47	49
57	49	12	13	17
48	58	50	16	41
51	59	51	42	50
52	60	52	43	51
53	61	53	44	52
54	62	54	45	53
55	63	55	46	54
56	64	56	47	55
57	65	57	48	56
58	66	58	17	49
57	67	59	16	50
60	68	60	51	59
61	69	61	52	60
62	70	62	53	61
63	71	63	54	62
64	72	64	55	63
65	73	65	56	64
66	74	66	57	65
67	75	67	17	58
66	76	68	20	59
69	77	69	60	68
70	78	70	61	69
71	79	71	62	70
72	80	72	63	71
73	81	73	64	72
74	82	74	65	73
75	83	75	66	74
76	84	76	21	67
75	85	77	20	68
78	86	78	69	77
79	87	79	70	78
80	88	80	71	79
81	89	81	72	80
82	90	82	73	81
83	91	83	74	82
84	92	84	75	83
85	93	85	21	76
84	94	86	20	77
87	95	87	78	86
88	96	88	79	87
89	97	89	80	88
90	98	90	81	89
91	99	91	82	90

92	100	92	83	91
93	101	93	84	92
94	102	94	21	85
93	103	95	24	86
96	104	96	87	95
97	105	97	88	96
98	106	98	89	97
99	107	99	90	98
100	108	100	91	99
101	109	101	92	100
102	110	102	93	101
103	111	103	25	94
102	112	104	24	95
105	113	105	96	104
106	114	106	97	105
107	115	107	98	106
108	116	108	99	107
109	117	109	100	108
110	118	110	101	109
111	119	111	102	110
112	120	112	25	103
111	121	113	24	28
29	104	114	114	29
105	113	115	115	29
106	114	116	116	30
107	115	117	117	30
108	116	118	118	30
109	117	119	119	31
110	118	120	120	31
111	119	121	121	25
31	32	112	120	